www.ietdl.org

Published in IET Microwaves, Antennas & Propagation
Received on 17th September 2012
Revised on 18th March 2013
Accepted on 17th June 2013
doi: 10.1049/iet-map.2012.0540

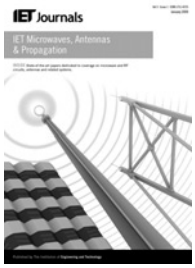

ISSN 1751-8725

Vibration sensitivity reduction of two microwave oscillators using inter-injection locking technique

Mohammad Reza Modarresi, Ali Banai, Forouhar Farzaneh

School of Electrical Engineering, Sharif University of Technology, P.O. Box 11155-4363, Tehran, Iran
E-mail: banai@sharif.edu

Abstract: Phase noise is one of the most important specifications of microwave oscillators. External factors such as mechanical vibrations increase the phase noise of the oscillator. A novel technique is introduced to reduce vibration-induced phase noise using inter-injection locking of two coupled oscillators. Two similar oscillators with equal free running frequencies are chosen and are subjected to sinusoidal vibration. The mechanical configuration is such that vibration sensitivity vector increases the frequency of one oscillator and decreases the other one's frequency of oscillation. Coupling these two oscillators using inter-injection locking, the common after-lock frequencies of both oscillators would be equal to the free running frequency of oscillation; as such the influence of vibration on the oscillators is reduced. Experimental measurements are carried out to confirm the proposed technique.

1 Introduction

Mechanical vibrations increase the phase noise of a microwave oscillator. This may be because of several parameters like resonator installation, elastic properties of resonator and other mechanical parts of the oscillator. Experimental studies have shown that the sensitivity of a resonator to either acceleration or vibration is a vector quantity. Vibration sensitivity of oscillators is explained in detail in [1–4]. If an oscillator with the acceleration sensitivity vector of $\boldsymbol{\Gamma}$ is subjected to the acceleration vector $\boldsymbol{a}$, its oscillation frequency will shift. Then, the oscillation frequency of vibrating oscillator is given by the following equation

$$f = f_0(1 + \boldsymbol{\Gamma}\,\boldsymbol{a}) \tag{1}$$

where f_0 is the frequency of the oscillation without acceleration. Equation (1) shows that if the acceleration sensitivity vector and the applied acceleration vector are in the same direction, the oscillation frequency shift will be maximised. The change in frequency depends on the sign of the inner product of the second term in (1).

2 Sinusoidal vibration study

2.1 Time domain study

A usual way of vibration study is assuming sinusoidal variation for the acceleration vector

$$\boldsymbol{a} = \boldsymbol{A}\cos(2\pi f_m t) \tag{2}$$

Then, the instantaneous frequency of an oscillator exposed to this vibration varies as in the following equation

$$f(t) = f_0\big(1 + (\boldsymbol{\Gamma}\,\boldsymbol{A})\cos(2\pi f_m t)\big) = f_0 + \Delta f\cos(2\pi f_m t) \tag{3}$$

Here, Δf is the maximum frequency deviation of the oscillator because of applied vibration and is expressed in terms of vector components as in the following equation

$$\Delta f = f_0\left(\Gamma_x A_x + \Gamma_y A_y + \Gamma_z A_z\right) \tag{4}$$

Using (3), the output voltage of the oscillator changes in the following equation

$$V(t) = V_0\cos\left(2\pi f_0 t + \left(\frac{\Delta f}{f_m}\right)\sin(2\pi f_m t)\right) \tag{5}$$

Equation (5) shows that if an oscillator is subjected to a sinusoidal vibration, the output voltage of the oscillator will be a frequency modulated signal.

2.2 Frequency domain study

Using the Bessel functions, the output voltage of the vibrating oscillator can be expanded in the following equation

$$\begin{aligned} V(t) = V_0[&J_0(\beta)\cos(2\pi f_0 t) \\ &+ J_1(\beta)\cos(2\pi(f_0 + f_m)t) \\ &+ J_1(\beta)\cos(2\pi(f_0 - f_m)t) \\ &+ J_2(\beta)\cos(2\pi(f_0 + 2f_m)t) \\ &+ J_2(\beta)\cos(2\pi(f_0 - 2f_m)t) + \cdots] \end{aligned} \tag{6}$$

In which β is the modulation index and is given by the following equation

$$\beta = \Delta f / f_m = (\boldsymbol{\Gamma}\, \boldsymbol{A}) f_0 / f_m \tag{7}$$

Equation (6) shows that sidebands are induced on the left-hand and right-hand sides at integer multiples of f_m offsets around the carrier. The relative levels (in dB) of these sidebands with respect to the carrier are

$$L(\text{dBc}) = 20\text{Log}\big(J_n(\beta)/J_0(\beta)\big) \tag{8}$$

For a low-modulation index ($\beta < 0.1$), that is, narrowband FM, one can use the approximations $J_0(\beta) \cong 1$, $J_1(\beta) \cong \beta/2$ and ignore higher order sidebands for $n \geq 2$.

So for a low-modulation index, the sidebands are only induced at the offset f_m from the carrier for which their relative levels are

$$L(\text{dBc}) = 20\text{Log}\left(\frac{(\boldsymbol{\Gamma}\, \boldsymbol{a}) f_0}{2 f_m}\right) = 20\text{Log}\left(\frac{\Delta f}{2 f_m}\right) \tag{9}$$

3 Inter-injection locking of coupled vibrating oscillators

In a similar way, random vibration increases the phase noise of an oscillator. The increased phase noise of oscillators can reduce the performance of the receivers and transmitters in many applications especially in mobile systems. Several methods have been proposed to reduce the undesirable effects of vibration on the oscillators [5, 6]. These techniques include selecting low-vibration-sensitive materials, active vibration cancellation schemes [6], using dampers [7–9], phase locking of references and bootstrapping of several oscillators [10].

Injection and inter-injection locking of oscillators are effective techniques to synchronise coupled oscillators either unilaterally or mutually. The equations governing the dynamic and steady-state behaviour of these techniques have been studied before in [11, 12], along with phase noise in these synchronised oscillators [13, 14, 19].

In this section, we will show that proper inter-injection locking of two vibrating microwave oscillators can reduce the effect of vibration on them. For this purpose, two similar oscillators with same free running frequencies are subjected to a sinusoidal vibration with vibration frequency f_m. The vibration sensitivity vector of the first oscillator has the same direction as the applied acceleration vector; $\boldsymbol{\Gamma}_1 = \boldsymbol{ca}$, and the vibration sensitivity vector of the second oscillator is in the opposite direction to this vector; $\boldsymbol{\Gamma}_2 = -\boldsymbol{ca}$. Hence, for the oscillators using $\boldsymbol{\Gamma}_1 = -\boldsymbol{\Gamma}_2 = \boldsymbol{\Gamma}$, one can write

$$\Delta f_1 = -\Delta f_2 = f_0 \boldsymbol{\Gamma}\, \boldsymbol{a} = f_0 |\boldsymbol{\Gamma}||\boldsymbol{a}| \tag{10}$$

If the two oscillators are similar, instantaneous frequencies of the vibrating oscillators become

$$f_1 = f_0 + \Delta f \cos(2\pi f_m t) \tag{11a}$$

$$f_2 = f_0 - \Delta f \cos(2\pi f_m t) \tag{11b}$$

Prior to study of the inter-injection locking of coupled vibrating oscillators, a circuit model for the vibrating oscillator is extracted.

3.1 Circuit model for a vibrating oscillator

First consider the series resonant circuit shown in Fig. 1, which represents the vibrating oscillator along with the active element and external injection source [15]. We put this external source in order to obtain formulae that will be used in the next section.

In this circuit, ΔL is time varying inductance that models the frequency variations of the oscillator because of vibration and V_{inj} represents the external injection from the mutually coupled oscillator to this oscillator. The phasor $\bar{A}$ stands for the loop current. The free running frequency of oscillation without any injection and vibration, is $f_0 = 1/2\pi\sqrt{LC}$. By exposing this oscillator to sinusoidal vibrations the instantaneous frequency changes to

$$f(t) = f_0 + \Delta f \cos(\omega_m t) = \frac{1}{2\pi\sqrt{(L + \Delta L)C}} \tag{12}$$

assuming $(\Delta L/L) \ll 1$ hence

$$\frac{1}{2\pi\sqrt{(L + \Delta L)C}} \cong f_0\left(1 - \frac{\Delta L}{2\,L}\right) = f_0 + \Delta f \cos(2\pi f_m t)$$

$$\Rightarrow \Delta L = \frac{-2\,L\Delta f}{f_0}\cos(2\pi f_m t) \tag{13}$$

We use this circuit model to explore the dynamic behaviour of two mutually coupled oscillators under vibration.

Defining time varying voltage phasor for output voltage of the vibrating oscillator is shown in Fig. 1, as

$$V = R_L A(t) e^{j\theta(t)} = R_L A(t) e^{j(2\pi f_0 t + \beta \sin \omega_m t)} \tag{14}$$

Then, writing the KVL in the oscillator loop [16], one obtains by the following equation

$$\frac{dV}{dt} = \frac{\pi f_0}{Q}\left(1 + \frac{\Delta f}{f_0}\cos \omega_m t\right) \times V_{\text{inj}} + \left(j2\pi f_0\left(1 + \frac{\Delta f}{f_0}\cos \omega_m t\right) - \frac{2\pi f_0}{Q}\left(1 + \frac{\Delta f}{f_0}\cos \omega_m t\right)\left(1 - \frac{R_D}{R_L}\right)\right) V \tag{15}$$

Separating the real and imaginary parts of this equation and

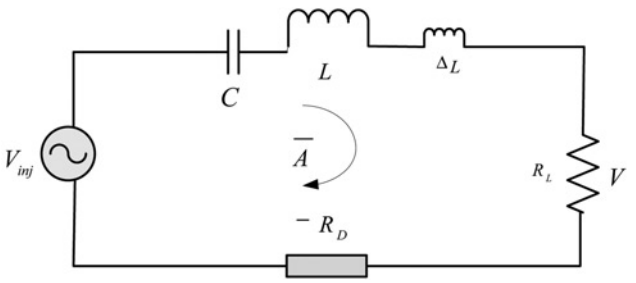

Fig. 1 *Equivalent circuit of a vibrating oscillator with external injection*

assuming $V_{\text{inj}} = \varepsilon R_L A_{\text{inj}}(t)e^{j\theta_{\text{inj}}(t)}$ one obtains the following equation

$$\begin{aligned}\frac{d\theta}{dt} &= \left(2\pi f_0 + 2\pi\Delta f\cos\omega_m t\right) + \frac{1}{2Q}\frac{A_{\text{inj}}}{A}\\ &\quad \left(2\pi f_0 + 2\pi\Delta f\cos\omega_m t\right)\sin\left(\theta_{\text{inj}} - \theta\right)\\ \frac{dA}{dt} &= -\frac{A}{Q}\left(2\pi f_0 + 2\pi\Delta f\cos\omega_m t\right)\left(1 - \frac{R_D}{R_L}\right)\\ &\quad + \frac{1}{2Q}\frac{A_{\text{inj}}}{A}\left(2\pi f_0 + 2\pi\Delta f\cos\omega_m t\right)\cos\left(\theta_{\text{inj}} - \theta\right)\end{aligned} \tag{16}$$

Without any external injection, $A_{\text{inj}} = 0$, from the phase equation we conclude that the FM sideband levels are smaller than the carrier by a factor $\gamma_{\text{single}} = \Delta f/2f_m$

3.2 Inter-injection locking of coupled oscillators under vibration

Now consider two similar oscillators with same free running frequencies coupled with each other. A circuit model for these two vibrating mutually coupled oscillators is proposed in Fig. 2 [15]. These two oscillators have been mutually coupled using a passive reciprocal circuit like an attenuator and a transmission line. In this circuit, ε and φ are the magnitude and the phase of the coupling coefficient of the coupling network, respectively, and the output voltages of the vibrating oscillators are

$$V_1(t) = R_L A_1(t)e^{j\theta_1(t)} \quad \text{and} \quad V_2(t) = R_L A_2(t)e^{j\theta_2(t)}$$

Assume that the acceleration vector and the acceleration sensitivity vector are in the same direction for the first oscillator and are in the opposite direction for the second one. Using (11) and (13) we have

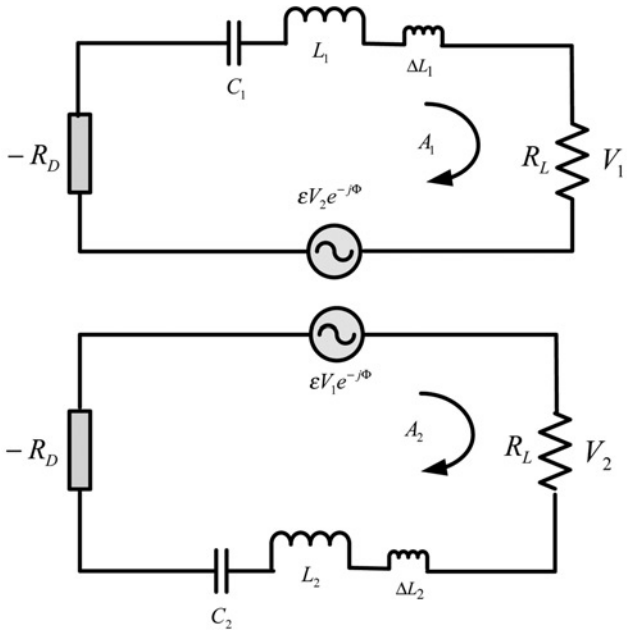

Fig. 2 *Circuit model for two mutually coupled vibrating oscillators*

$\Delta L_1 = -\Delta L_2 = \dfrac{-2\,L\Delta f}{f_0}\cos\left(2\pi f_m t\right)$ Assuming that a small part of the voltage of one oscillator is injected into the other oscillator (weak coupling), then for coupling phase equal to 2π, one obtains

$$\begin{aligned}V_{\text{inj},1}(t) &= \varepsilon R_L A_2(t)e^{j\theta_2(t)}\\ V_{\text{inj},2}(t) &= \varepsilon R_L A_1(t)e^{j\theta_1(t)}\end{aligned} \tag{17}$$

For each oscillator, a differential equation [similar to (15)] describes the time variations of complex phasor V of the oscillator. Substituting voltages V_1 and V_2 from (17) in (15) and separating real and imaginary parts of these equations one obtains four coupled non-linear differential equations governing the amplitudes and the phases of these oscillators by the following equations

$$\frac{d\theta_1}{dt} = \left(2\pi f_0 + 2\pi\Delta f\cos\omega_m t\right) + \frac{\varepsilon}{2Q}\frac{A_2}{A_1} \times \left(2\pi f_0 + 2\pi\Delta f\cos\omega_m t\right)\sin\left(\theta_2 - \theta_1\right) \tag{18a}$$

$$\frac{d\theta_2}{dt} = \left(2\pi f_0 - 2\pi\Delta f\cos\omega_m t\right) + \frac{\varepsilon}{2Q}\frac{A_1}{A_2} \times \left(2\pi f_0 - 2\pi\Delta f\cos\omega_m t\right)\sin\left(\theta_1 - \theta_2\right) \tag{18b}$$

$$\frac{dA_1}{dt} = -\frac{A_1}{Q}\left(2\pi f_0 + 2\pi\Delta f\cos\omega_m t\right)\left(1 - \frac{R_D}{R_L}\right) + \frac{\varepsilon A_2}{2Q}\left(2\pi f_0 + 2\pi\Delta f\cos\omega_m t\right)\cos\left(\theta_2 - \theta_1\right) \tag{18c}$$

$$\frac{dA_2}{dt} = -\frac{A_2}{Q}\left(2\pi f_0 - 2\pi\Delta f\cos\omega_m t\right)\left(1 - \frac{R_D}{R_L}\right) + \frac{\varepsilon A_1}{2Q}\left(2\pi f_0 - 2\pi\Delta f\cos\omega_m t\right)\cos\left(\theta_1 - \theta_2\right) \tag{18d}$$

where Q stands for loaded quality factor of the oscillators; $Q = \omega_0 L/R_L$.

However, since the injection level in the oscillator loop is small ($\varepsilon \ll 1$), the amplitudes do not change considerably and the dynamics of the oscillators can be well described only by the phase differential equations [15, 16]. By this assumption, the phase equations are decoupled from amplitude equations. As such, the phase variations of $\theta_1(t)$ and $\theta_2(t)$ are explained by the following equations:

$$\frac{d\theta_1}{dt} = \left(2\pi f_0 + 2\pi\Delta f\cos\omega_m t\right) + \frac{\varepsilon}{2Q} \times \left(2\pi f_0 + 2\pi\Delta f\cos\omega_m t\right)\sin\left(\theta_2 - \theta_1\right) \tag{19a}$$

$$\frac{d\theta_2}{dt} = \left(2\pi f_0 - 2\pi\Delta f\cos\omega_m t\right) + \frac{\varepsilon}{2Q} \times \left(2\pi f_0 - 2\pi\Delta f\cos\omega_m t\right)\sin\left(\theta_1 - \theta_2\right) \tag{19b}$$

Subtracting (19b) from (19a) and defining the phase difference $\psi(t) = \theta_1(t) - \theta_2(t)$, we obtain

$$\frac{d\psi(t)}{dt} = 4\pi\Delta f\cos\left(\omega_m t\right) - \frac{\varepsilon}{Q}2\pi f_0\sin\psi(t) \tag{20}$$

Since $\psi(t)$ is small for oscillators under vibration, the $\sin(\psi(t))$

doi: 10.1049/iet-map.2012.0540

term can be approximated by its argument, hence, the solution of (20) becomes

$$\psi(t) = \alpha\cos(\omega_m t) + \zeta\sin(\omega_m t) \tag{21}$$

In which

$$\alpha = \frac{K\zeta}{f_m}, \quad \zeta = \frac{4\pi f_m \Delta f}{K^2 + f_m^2}$$

where K is an auxiliary variable and is equal to $K = (\varepsilon f_0/Q)$.

For small $\psi(t)$ (18a) is rewritten as

$$\begin{aligned}\frac{\mathrm{d}\theta_1(t)}{\mathrm{d}t} &= (2\pi f_0 + 2\pi\Delta f\cos\omega_m t)\\ &\quad - \frac{\varepsilon}{2Q}(2\pi f_0 + 2\pi\Delta f\cos\omega_m t)\psi(t)\end{aligned} \tag{22}$$

After substituting (21) in (22) we arrive at the following equation

$$\begin{aligned}\frac{\mathrm{d}\theta_1(t)}{\mathrm{d}t} &= \left[\left(2\pi f_0 - \frac{\pi\varepsilon\alpha\Delta f}{2Q}\right)\right]\\ &\quad + \left[\left(2\pi\Delta f - \frac{\varepsilon\pi\alpha f_0}{Q}\right)\cos(\omega_m t) - \frac{\varepsilon\zeta\pi f_0}{Q}\sin(\omega_m t)\right]\\ &\quad - \left[\frac{\varepsilon\alpha\pi\Delta f}{2Q}\cos(2\omega_m t) + \frac{\varepsilon\zeta\pi\Delta f}{2Q}\sin(2\omega_m t)\right]\end{aligned} \tag{23}$$

In (23), the first bracket represents the after lock carrier frequency of the vibrating oscillator, whereas the second and third brackets are representing the generated sidebands at f_m and $2f_m$ offset from the carrier, respectively. Since $\Delta f \ll f_0$, we conclude that the sidebands at $2f_m$ are much smaller than those at f_m, hence, we consider only the $f_0 + f_m$ and $f_0 - f_m$ sidebands afterwards. To calculate the amplitude of these sidebands we rewrite the terms in the second bracket of (23) in a closed sinusoidal form

$$\begin{aligned}&\left(2\pi\Delta f - \frac{\varepsilon\pi\alpha f_0}{Q}\right)\cos(\omega_m t) - \frac{\varepsilon\pi\zeta f_0}{Q}\sin(\omega_m t)\\ &\quad = \gamma_{\text{coupled}}\cos(\omega_m t + \eta)\end{aligned} \tag{24}$$

Using simple trigonometric relations, one obtains the following equation

$$\gamma_{\text{coupled}} = 2\pi\Delta f\sqrt{1 - \frac{K^2}{K^2 + f_m^2}} = \frac{2\pi\Delta f\, f_m}{\sqrt{K^2 + f_m^2}} \tag{25}$$

Rewriting the simplified form of (23) (neglecting the sidebands induced at $2f_m$) we arrive at the following equation

$$\frac{\mathrm{d}\theta_1(t)}{\mathrm{d}t} = \left(2\pi f_0 - \frac{\varepsilon\pi\Delta f}{2Q}\right) + \gamma_{\text{coupled}}\cos(\omega_m t + \eta) \tag{26}$$

As is apparent from (26), the output voltage of the first oscillator (and similarly that of the second one) is an FM modulated signal with a modulation index of $\beta_{\text{coupled}} = (\gamma_{\text{coupled}}/\omega_m)$.

Assuming narrowband FM in the same manner as described in Section 2, the level of the sidebands induced at $f_0 + f_m$ and $f_0 - f_m$ relative to the carrier after inter-injection locking is obtained by the following equation

$$\begin{aligned}L_{\text{coupled}}(\text{dBc}) &= 20\text{Log}\left(\frac{\gamma_{\text{coupled}}}{2\omega_m}\right)\\ &= 20\text{Log}\left(\frac{\Delta f}{2\sqrt{K^2 + f_m^2}}\right)\end{aligned} \tag{27}$$

Now, we should compare the level of the induced sidebands at f_m offset from the carrier in the coupled vibrating oscillators with that of a single vibrating oscillator. We define reduction factor as the relative difference of sidebands between these two cases, using (9) and (27) we have

$$\text{reduction factor (dB)} = 20\text{Log}\left(\frac{f_m}{\sqrt{K^2 + f_m^2}}\right) \tag{28}$$

The reduction factor is plotted in Fig. 3 for a 1 GHz oscillator with $Q = 50$ for two coupling factors of $\varepsilon = 0.2$, against modulation frequency. It is easy to show that the second oscillator has the same spectrum as the first oscillator.

As is apparent from Fig. 3, after inter-injection locking of two vibrating oscillators, induced sidebands at $f_0 + f_m$ and $f_0 - f_m$ become very small.

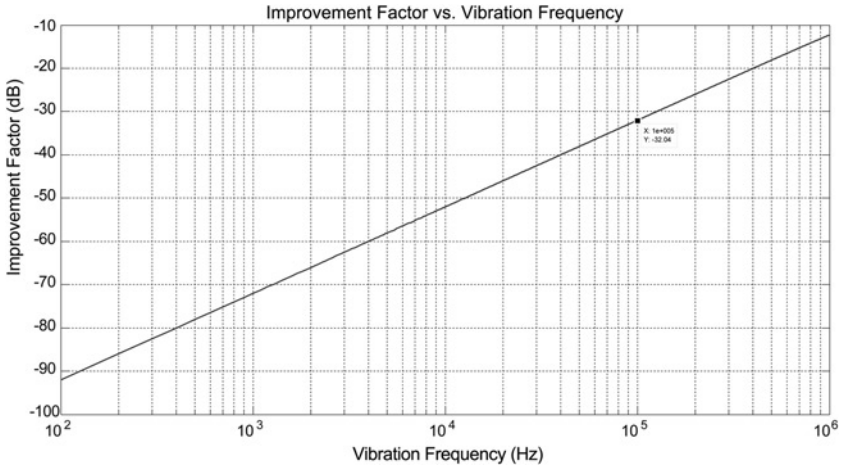

Fig. 3 *Reduction factor (dB) against modulation frequency (Hz)*

An intuitive interpretation for the reason of spurious reduction can be explained as the following:

We have two oscillators if there were no coupling between them the effect of vibration is pulling up the frequency of one of these oscillators and pulling down the other exactly by the same amount. Now, establishment of a coupling between these two oscillators causes them to pull each other oppositely whereas the common frequency of oscillation remains constant equal to f_0 which is the average of f_0+f_m and f_0-f_m that is f_0 [15]. In other words, the oscillators are not free as before; each oscillator is forced to change the frequency of the other in the opposite direction of the acceleration vector.

In the real world, the spectrum of the vibration is usually spread over a frequency range; by using the proposed method, the phase noise of the oscillators around the carrier will be reduced in a similar manner.

4 Measurement results

In this section, the experimental measurements on microwave vibrating oscillators using inter-injection locking method will be explained. We used two similar dielectric resonator oscillators at 10 GHz frequency band for this purpose. The dielectric resonator oscillators (DRO) are fabricated using FMM5201 monolithic microwave integrated circuit (MMIC), from Eudyna, which is a dual element GaAs FET and one element is used for our DR oscillator [17]. This MMIC shows negative resistance in a broad frequency range from 9.75 to 11.5 GHz. The block diagram of the oscillator is shown in Fig. 4. Indeed, we used ready DROs from low noise block (LNB) down converter of commercial satellite receivers.

Three axes can be defined for one DRO according to the mounting plane of the dielectric resonator. The x- and y-axes are defined in the plane of PCB and z-axis is defined perpendicular to it (see Fig. 5*a*). Measurements show that the acceleration sensitivity of the DRO is much greater in z-axis compared with the x- and y-axes. For example, the acceleration sensitivity for the z-axis in a DRO can be an order of magnitude greater than the other axes [18].

The two oscillators are mutually coupled as depicted in Fig. 6. The magnitude of coupling coefficient is fixed and determined by the coupling factors of directional couplers, which are 10 dB couplers here. However, a line stretcher was used to adjust the phase of the coupling to multiples of 360°. We fixed these oscillators in several configurations (Fig. 5*b*) and vibrated them together. The oscillators are vibrated using a standard shaker system. The shaker is a computer controlled system whose acceleration frequency and amplitude are controllable from 100 Hz to 10 kHz and from 1 to 100 g's, respectively. This shaker exerts the

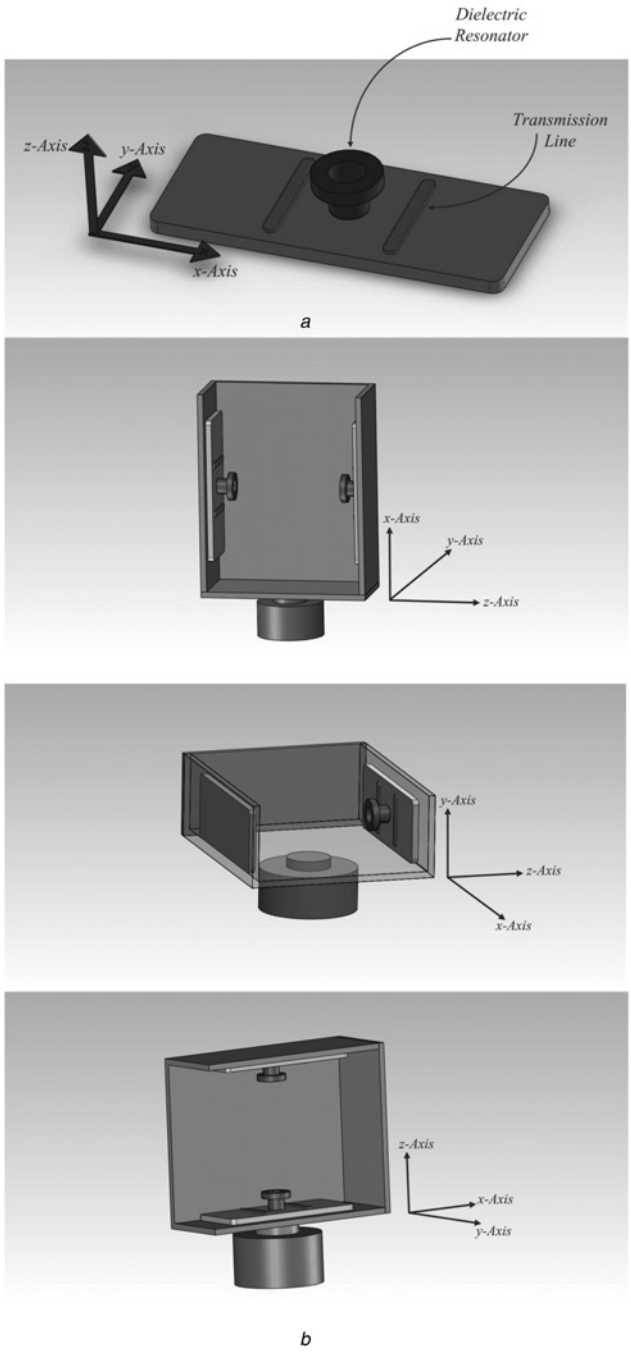

Fig. 5 *x- and y-axes are defined in the plane of PCB and z-axis is defined perpendicular*

a DRO's cordinates
b Three ways for vibrating two mutually coupled DROs (x, y and z, respectively)

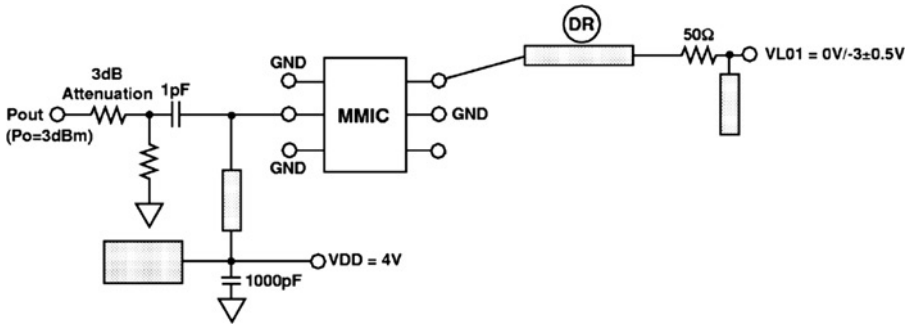

Fig. 4 *Block diagram of the GaAs FET MMIC oscillator*

doi: 10.1049/iet-map.2012.0540

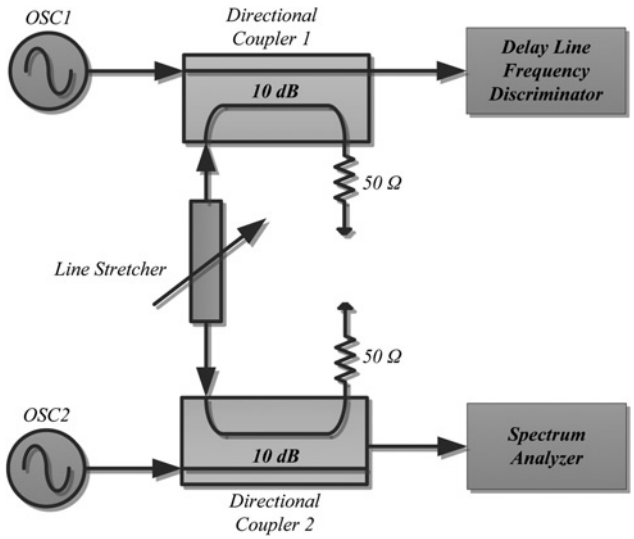

Fig. 6 *Block diagram of two inter-injection locked oscillators*

defined acceleration in the direction perpendicular to its top sheet where the oscillators' fixture is tightly fixed. The direct ports of the couplers are connected to the spectrum analyser and the phase noise measurement system.

Since the oscillators are not stable enough to read sideband levels directly from the spectrum analyser, we used a phase noise measurement system based on delay-line frequency discrimination technique to extract the spurious levels of vibrating oscillators [19]. The block diagram of the phase noise measurement system is shown in Fig. 7. In our experiments, the absolute value of spurious is not important, but relative reduction of this spurious before and after inter-injection locking of oscillators is our main concern.

The measured spectrums of the single free running oscillator are shown in Figs. 8*a* and *b*. The spurious in this figure are AC power supply harmonics. First, this oscillator vibrated by 5 g, 1 kHz sinusoidal vibration in the direction of *z*-axis, the spectrums of the vibrating oscillator are shown in Figs. 9*a* and *b*.

The experiment was repeated for *x*- and *y*-axes as well, we observed that the acceleration sensitivity vector is about 6 dB smaller than *z*-direction for these axes meaning that the acceleration sensitivity vector of the DRO has negligible components in *x*- and *y*-directions. As such we can assume that the acceleration vectors of these oscillators are approximately parallel to *z*-axis.

Now, according to the block diagram of Fig. 6, two oscillators were mounted and fixed on the fixture in three configurations (shown in Fig. 5*b*) and exposed to vibration. The oscillators are put on opposite sides along the *z*-axis. The after-lock spectrum of the coupled oscillators subjected to vibration in the direction of *z*-axis is shown in Fig. 10. The reduction of 1 kHz spurious according to these measurements is about 8 dB. The measured reduction in 1 kHz sideband is not in the order of prediction of Section 3. The main reason is that the reduction factor of (28) is valid only when two oscillators have exactly the same characteristics, however, simulation can be performed to reveal that inter-injection coupling of non-similar oscillators (non-similar frequency of oscillation, output power and acceleration sensitivity) degrades the reduction factor substantially. In the next section, we show through the dynamic simulation of two oscillators with slightly different characteristics, how the expected sideband reduction factor could be reduced significantly.

5 Dynamic simulation and discussion

It is observed that reduction in the spurious sidebands is far less than the expected theoretical values described by (28), here we discuss how and why practical sideband reduction could be in the vicinity of the measured values. Consider (18), these differential equations describe the dynamic behaviour of two mutually coupled oscillators. It is common to assume a quadratic behaviour for non-linear resistance (R_D) to model the non-linearity (Van der Pol oscillator)

$$\left(1-\frac{R_D}{R_L}\right)=\mu\left(|A|^2-|A_0|^2\right) \tag{29}$$

In which A_0 is the free running amplitude of oscillation and μ is an empirical constant which models the saturation behaviour of the non-linear element. We have chosen $\mu=3$ in our simulations. Applying this model, (18a) and (18b) become

$$\frac{\mathrm{d}A_1(t)}{\mathrm{d}t}=\frac{\mu}{2Q}\left(2\pi f_0+2\pi\Delta f\cos\omega_m t\right)A_1\left(A_0^2-A_1^2\right)+\frac{\varepsilon}{2Q}\left(2\pi f_0+2\pi\Delta f\cos\omega_m t\right)A_2\cos\left(\theta_2-\theta_1\right) \tag{30}$$

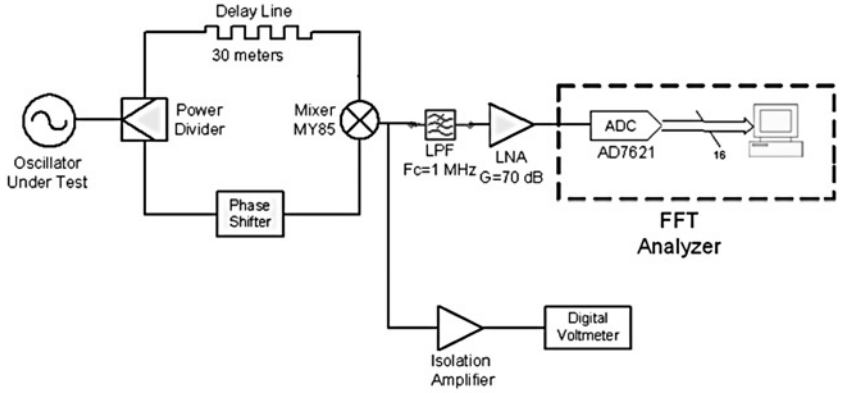

Fig. 7 *Block diagram of the phase noise measurement system [19]*

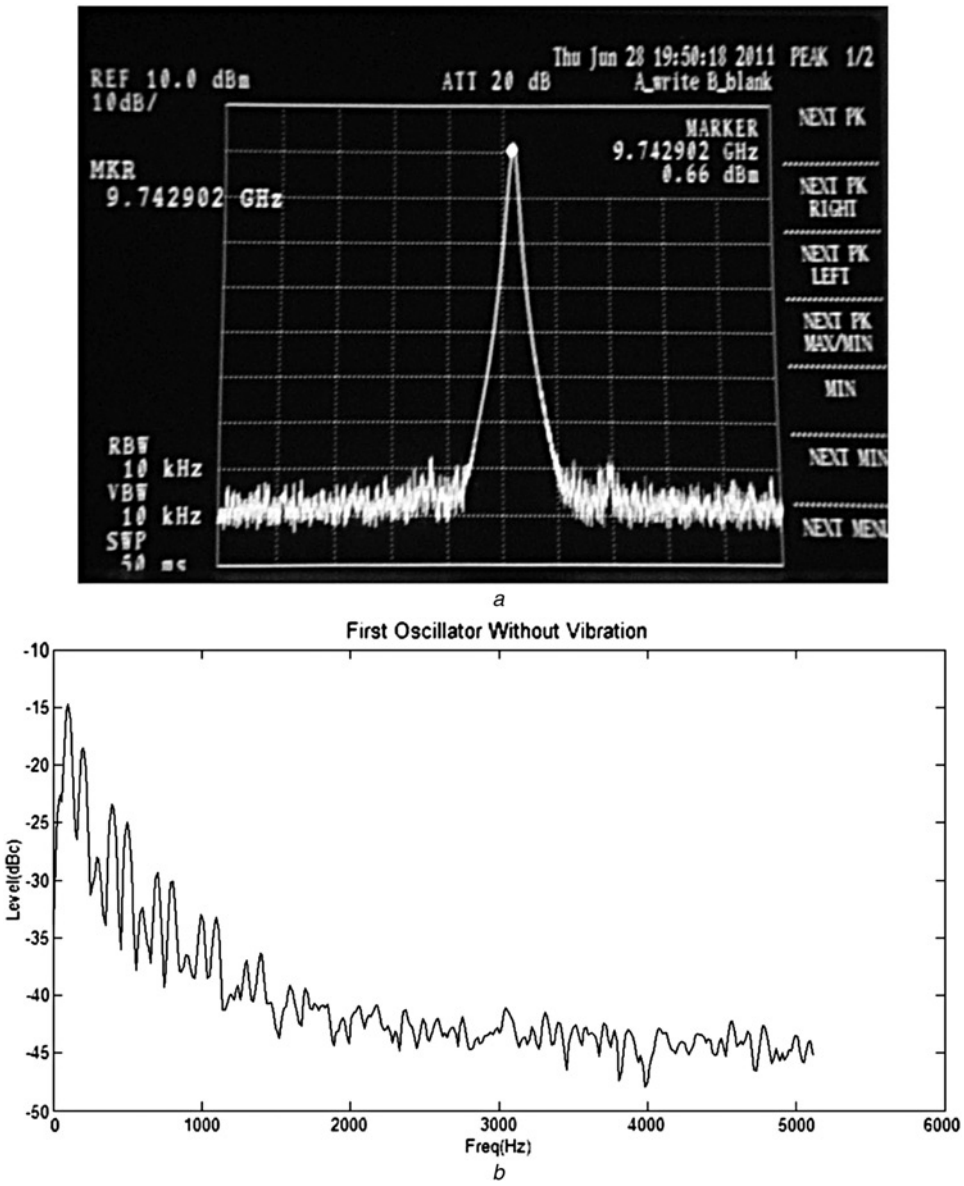

Fig. 8 *Measured spectrums of the single free running oscillator*

a Spectrum of the non-vibrating oscillator
b Spectrum of the non-vibrating oscillator measured by delay line frequency discriminator

$$\frac{\mathrm{d}A_2(t)}{\mathrm{d}t} = \frac{\mu}{2Q}\left(2\pi f_0 - 2\pi\Delta f\cos\omega_m t\right)A_2\left(A_0^2 - A_2^2\right) + \frac{\varepsilon}{2Q}\left(2\pi f_0 - 2\pi\Delta f\cos\omega_m t\right)A_1\cos\left(\theta_1 - \theta_2\right) \tag{31}$$

The phase equations remain unchanged. Although it is true that the phase equations are dominant for specifying the behaviour of weakly coupled oscillators (as we assumed in Section 3), here we consider both phase and amplitude equations. As such we can also see the effect of non-equal amplitudes of coupled oscillators on the sidebands reduction factor. Numerical simulations confirm that the contribution of amplitude discrepancy can be ignored.

We solve these non-linear equations numerically (using Runge–Kutta numerical solver of MATLAB) and obtain the amplitude and phase of each oscillator against time. Then, using fast Fourier transform (FFT) algorithm, the frequency spectrum of oscillators can be obtained.

We choose $f_0 = 1$ GHz as free running oscillation frequency, $f_m = 100$ kHz as vibration frequency, $Q = 50$ as loaded quality factors of oscillators and $|\Gamma| = 1 \times 10^{-5}/g$ as the magnitude of the acceleration sensitivity vector and the coupling factor of $\varepsilon = 0.2$. Let us first obtain the output spectrum of a single oscillator subjected to acceleration. Assume $|\boldsymbol{a}| = 5$ g (parallel to the acceleration sensitivity vector). We have $\Delta f = f_0\ \boldsymbol{\Gamma a} = f_0|\boldsymbol{\Gamma}| \times |\boldsymbol{a}| = 10^9 \times 5 \times 10^{-5} = 5 \times 10^4$ Hz. The output spectrum of such a single vibrating oscillator is plotted in Fig. 11.

As can be seen from Fig. 11, the side bands induced by vibrating signal are about 13 dB below the carrier level and is consistent with the result of (9), which is about 12 dB.

Next, consider two coupled oscillators which are subjected to an acceleration vector $\vec{a}$ such that the vibration sensitivity vector of the first oscillator has the same direction as the

doi: 10.1049/iet-map.2012.0540

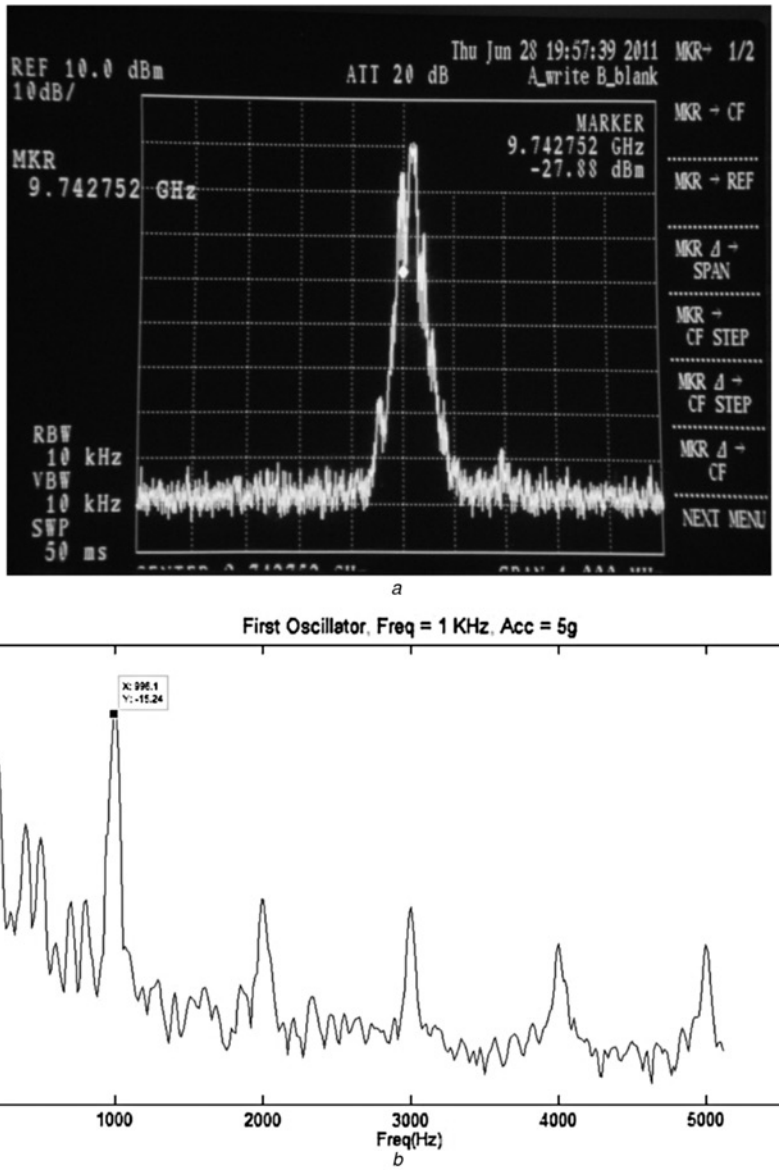

Fig. 9 *Spectrum of the oscillator vibrated by 5 g, 1 kHz sinusoidal vibration in the direction of z-axis*

a Spectrum of the single vibrating oscillator
b Spectrum of the vibrating oscillator measured by delay line frequency discriminator

applied acceleration vector; $\boldsymbol{\Gamma}_1 = \boldsymbol{ca}$, and the vibration sensitivity vector of the second oscillator is in the opposite direction to this vector; $\boldsymbol{\Gamma}_2 = -\boldsymbol{ca}$. First assume that the two oscillators are exactly similar. It means that their free running oscillation frequencies (f_0) and amplitudes (A_0), the magnitude and direction of their acceleration sensitivity vectors are the same exactly. The applied acceleration vector is the same as the previous example used for single oscillator. Now, four coupled nonlinear differential equations are solved numerically to obtain the phases and the amplitudes of the vibrating oscillators. The after lock output spectrum of one of the coupled oscillators is plotted in Fig. 12.

The reduction factor for these two coupled oscillators is plotted in Fig. 3 against vibration frequency. Comparing Figs. 3 and 11 shows that the reduction of side band level is close to the reduction factor predicted by (28). The difference between the results is mainly because of the following reasons:

- Since the injection level to each oscillator is small we supposed that the amplitudes of oscillators remain unchanged, and this permits us to ignore amplitude differential equations.
- The simplifications made to the phase equations (that is approximating sinusoid function with its argument).
- The assumption of narrowband FM, which is not complied well for the above simulated example.

In order to investigate the effect of discrepancies between two oscillators, we intentionally make differences in their characteristics. The main sources of discrepancies are

- Different acceleration sensitivity vectors (both magnitude and direction) of the oscillators which results in different modulation index

$$\beta_1 = \frac{\Delta f_1}{f_m} = \frac{f_0 \boldsymbol{\Gamma}_1\, a}{f_m} \quad \text{and} \quad \beta_2 = \frac{\Delta f_2}{f_m} = \frac{f_0 \boldsymbol{\Gamma}_2\, a}{f_m}$$

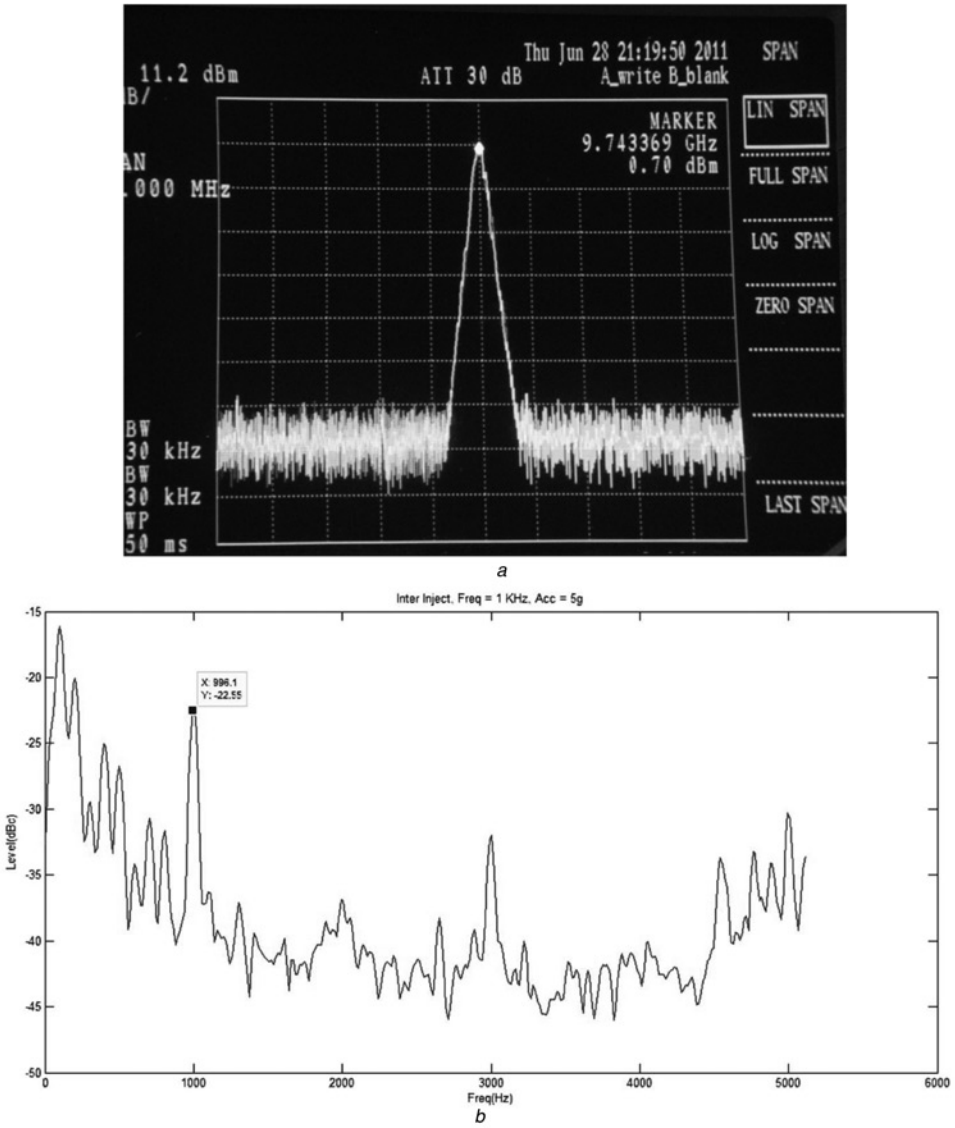

Fig. 10 *After-lock spectrum of the coupled oscillators subjected to vibration in the direction of z-axis*

a After-lock spectrum of vibrating oscillator 1
b After-lock spectrum of vibrating oscillators using delay line frequency discriminator

of the oscillators.

- Different free running frequencies of oscillation.
- Different free running amplitudes of oscillation.

Numerical simulations reveal that the dominant factor in degrading the sideband reduction, is different acceleration sensitivity vectors (different magnitude and direction) of the oscillators. This discrepancy could happen easily because of mechanically imperfect fabrication of oscillators or different position of the tuning screws of DROs. As an example, we assumed two oscillators with different modulation indices of 50%, $\beta_2 = 1.5\beta_1$, different free running frequencies of about 3 MHz (0.3%) and different free running amplitudes of about 2 dB. The resultant output spectrum of one of the inter-injection locked oscillators, after numerical computation, is plotted in Fig. 13.

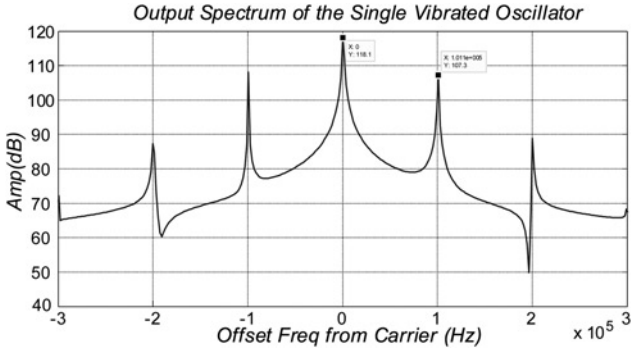

Fig. 11 *Output spectrum of a single vibrating oscillator*

Fig. 13 reveals that the reduction factor could be degraded by about 25 dB because of non-similarity of vibrating oscillators. This imperfection factors decreases the reduction factor to about 11 dB instead of the expected theoretical value of 36 dB. This reduction factor is in the order of values obtained in our measurement system.

6 Conclusion

Vibrations increase the phase noise of microwave oscillators. In this paper, a novel technique was proposed to reduce the undesirable effects of vibrations, that is by using

doi: 10.1049/iet-map.2012.0540

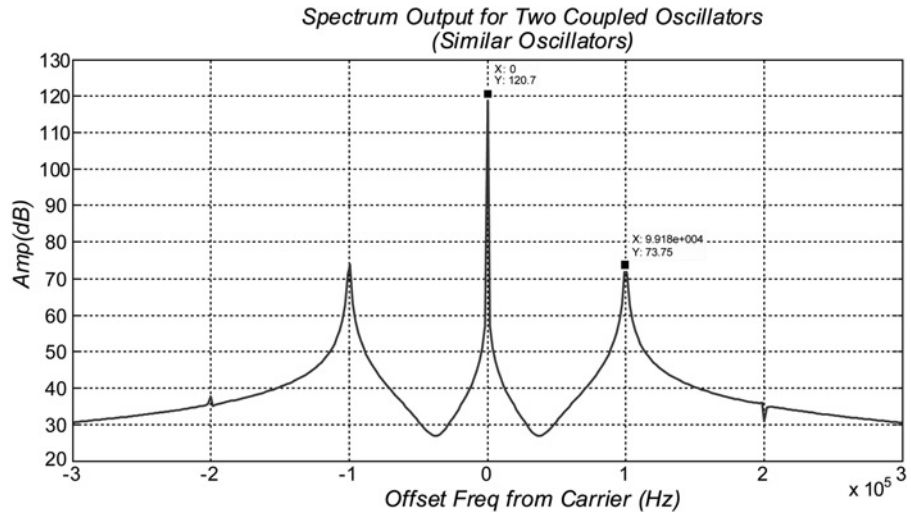

Fig. 12 *After lock output spectrum of two similar oscillators subjected to an acceleration vector*

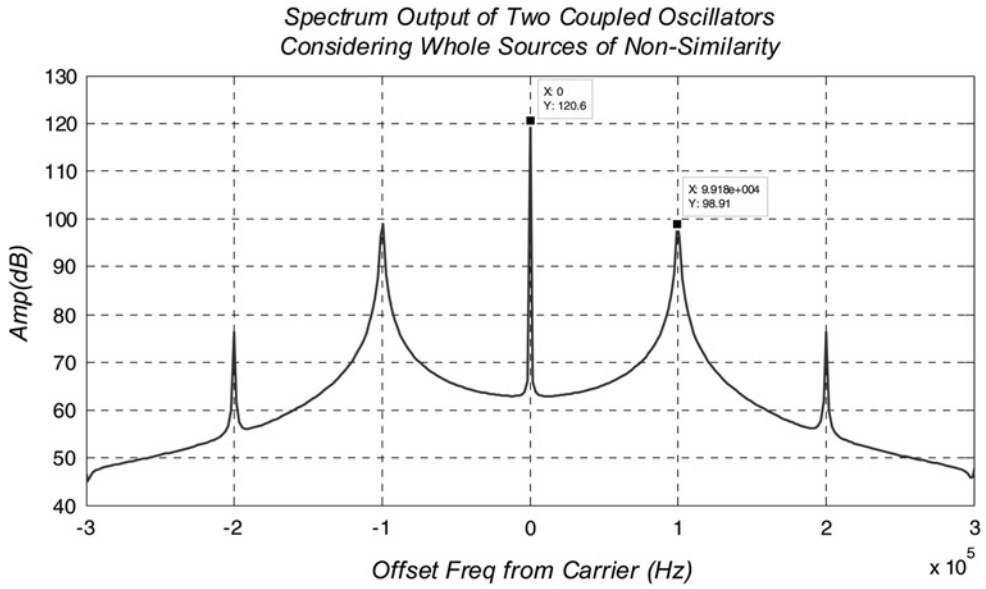

Fig. 13 *Reduction factor degradation because of considering all sources of discrepancy (frequency, amplitude and modulation index) of the coupled oscillators*

inter-injection locking of two mutually coupled oscillators. The oscillators must be placed in such a way as to have opposite acceleration sensitivity vectors. A theoretical formula was obtained for sideband reduction of vibrating coupled oscillators. However, dynamic simulations showed that reaching the theoretical reduction in sideband is improbable in practice, but one can expect sideband reduction of about one order lower in magnitude, which is still noticeable. Experimental measurements using sinusoidal vibration confirm the applicability of the proposed method and about 8 dB reduction in spurious of the vibrating oscillator was observed. The same reduction in augmented phase noise because of random vibration is expected.

7 References

1 Filler, R.L.: 'The acceleration sensitivity of quartz crystal oscillators: a review', *IEEE Trans. Ultrason. Ferroelectr. Freq. Control*, 1998, **35**, (3), pp. 297–305

2 Johnson, G.F.: 'Vibration characteristics of crystal oscillators'. Proc. 21st Annual Symp. Frequency Control, 1967, pp. 287–293

3 Sinha, B.K., Locke, S.: 'Acceleration and vibration sensitivity of SAW devices', *IEEE Trans. Ultrason. Ferroelectr. Freq. Control*, 1987, **34**, (1), pp. 29–38

4 Vig, J.: 'An overview of effects of vibration on phase noise'. 1st DARPA APROPOS Planning Meeting, Boulder, CO, January 2003

5 Kosinski, J.A.: 'Theory and design of crystal oscillators immune to acceleration: present state of the art'. IEEE Frequency Control Symp. and Exhibition Proc., June 2000, pp. 260–268

6 Hati, A., Nelson, C.W., Howe, D.A., *et al.*: 'Vibration sensitivity of microwave component'. IEEE Frequency Control Symp., June 2007, pp. 541–546

7 Nelson, C.L.: 'Reducing phase noise degradation due to vibration of crystal oscillators', Master of science thesis, Iowa State University, 2010

8 Wenzel Associates, Inc.:'Vibration-Induced Phase Noise', available at http://www.wenzel.com/documents/vibration.html, 10 December 2009

9 Aeroflex: 'Isolators for shock and vibration protection in all environments', Datasheet, 2M 1/2001

10 Wenzel C.: 'Bootstrapping a Phase Locked Loop for Better Performance'. Wenzel Associates, Inc., available at http://www.wenzel.com/pdffiles1/pdfs/bootstrp.pdf, 1994

11 Adler, A.: 'A study of locking phenomena in oscillators', *Proc. IEEE*, 1973, **61**, (10), pp. 1380–1385

12 Kurokawa, K.: 'Injection locking of microwave solid-state oscillators', *Proc. IEEE*, 1973, **61**, (10), pp. 1386–1410
13 Kurokawa, K.: 'Noise in synchronized oscillators', *IEEE Trans. Microw. Theory Tech.*, 1972, **16**, (4), pp. 234–240
14 Chang, X., Cao, H.C., Vaughan, M., Mishra, U.K., York, R.A.: 'Phase noise in coupled oscillators: theory and experiments', *IEEE Trans. Microw. Theory Tech.*, 1997, **45**, (5), pp. 604–615
15 Banai, A., Farzaneh, F.: 'Locked and unlocked behavior of mutually coupled microwave oscillators', *IEE Proc. Microw. Antennas Propag.*, 2000, **147**, (1), pp. 13–18
16 York, R.A., Compton, R.C.: 'Nonlinear analysis of phase relationships in quasi-optical oscillator arrays', *IEEE Trans. Microw. Theory Tech.*, 1993, **MTT-41**, (10), pp. 1799–1809
17 Eudyna: 'FMM5201MLT4E1 MMIC GaAs Dual Oscillator', Rev.2.0, 2005
18 Hati, A., Nelson, C., Howe, D.: 'Vibration-induced PM noise in oscillators and its suppression in Aerial Vehicles' (InTech, 2009) ch. 13, pp. 259–286
19 Nick, M., Banai, A., Farzaneh, F.: 'Phase noise measurement using two inter-injection locked microwave oscillators', *Trans. Microw. Theory Tech.*, 2006, **54**, (7), pp. 2993–3000

doi: 10.1049/iet-map.2012.0540